Cosmic Masers: Proper Motion toward the Next-Generation Large Projects
Proceedings IAU Symposium No. 380, 2024
T. Hirota, H. Imai, K. Menten, & Y. Pihlström, eds.
doi:10.1017/S1743921323002296

Simultaneous observations of exited OH and methanol maser - coincidence and magnetic field

Agnieszka Kobak

Institute of Astronomy, Nicolaus Copernicus University in Torun.
email: akobak@astro.uni.torun.pl

Abstract. We present the first results of simultaneous observations of the 6.035 GHz exited OH and 6.7 GHz methanol masers toward a sample of 10 high-mass young stellar objects (HMYSOs), observed using eMERLIN in 2020 and 2022. Searching for the coincidence and avoidance of these two maser transitions, we estimate physical conditions around central protostars. We identify Zeeman-splittings of the OH emission and determine the strength of the magnetic field. Combining it with linear polarization, we derive the magnetic field structure in these high-mass star-forming regions.

Keywords. methanol, exited OH, maser, magnetic field

1. Introduction

Astrophysical masers are one of the most important tools to study high-mass young stellar objects (HMYSOs). Due to masers, we can study, obscured by dense gas, regions around HMYSO. The most common species is methanol maser (6.7 GHz), which was widely studied by single-dish long-term observations (Szymczak *et al.* 2002); Szymczak *et al.* (2018); (Yang *et al.* 2019) as well as by interferometric observations during a few epochs (Bartkiewicz *et al.* 2009,K). Another kind of maser is exited OH (6.035 GHz, so-called ex-OH). These two transitions require specific physical conditions (Cragg *et al.* 2002). Methanol masers need a dust temperature (T_D) above 100 K and a gas temperature (T_K) below 200 K, whereby the maser diminishes when T_K exceed T_D. Masers appear in gas densities (ρ_{H_2}) between $10^{5.5}$ to $10^{7.5}$ cm^{-3}. Whereas the ex-OH maser arises in the cooler region at T_D above 20 K and T_K below 70 K, and these two parameters are independent. The gas density required for the existence of the 6.035 GHz transition is bigger, 10^6-$10^{8.5}$ cm^{-3}.

An important phenomenon during star formation is a magnetic field, which influences the star formation rate and fragmentation process (Krumholz & Federrath 2019). The strength of the magnetic field can be also a signature of the gas density according to the dependence B$\sim$n$^{0.4}$ (Garay *et al.* 1996). To estimate the strength of the magnetic field, the splitting of spectral lines (Zeeman splitting) is used. Because the OH molecule is paramagnetic, the splitting between velocity in left- and right-hand circular polarization (LHCP, RHCP) (V_Z) is significant and relatively easy to measure. To calculate the value of the magnetic field (B) we used the formula $\Delta V_Z/B = 0.056$ Baudry *et al.* (1997), with a value of 0.056 for the g-factor for the OH molecule. Using this method the magnetic field was examined for example for source W75N (Bartkiewicz *et al.* 2005) and for ON1 (Green *et al.* 2007).

In this paper, we present the result of the two sources G43.149+0.013 (hereafter G43) and G48.990−0.299 (hereafter G48). The observations were a part of the project CY10206, and were made using e-Merlin in 2020 and 2022. G43 is part of the vast star-forming region W49N. The far kinematic distance for this source is 10.96±0.35 kpc with 99% probability, for a central velocity 12 km s^{-1}(calculated using the parallax-based distance calculator V2 from Reid *et al.* (2019)). The G48 source lies at the kinematic distance of 5.44±0.47 kpc Reid *et al.* (2019).

2. Results

Results for these sources are presented in Figure 1. Both sources characterize more extended spatial emission of ex-OH than that of the methanol masers.

2.1. *G43.149+0.013*

In this source ex-OH maser emission covers an area of 280×250 mas (3070×2740 au) and a range of velocity 9.5–14.5 km s^{-1}. The methanol maser emission appears in the red-shifted part of the 6.035 GHz spectrum in the range from 13 km s^{-1}to 14.2 km s^{-1}and is spread over 150×110 mas (1650×1200 au). The spatial distribution of methanol maser is more compact than that of ex-OH, but it is more than 5 times brighter. The 6.7 GHz emission emerges in three groups, and these all coincide with the 6.035 GHz emission in both velocity and angular position, within 0.4 km s^{-1}and 25 mas. On the southeast side only extended ex-OH emission appears with a linear structure.

We identify eight Zeeman pairs at the 6.035 GHz transition. Pairs in the east have a positive magnetic field value equal to +3.2 mG and +3.7 mG, indicating that the magnetic field vectors are directed away from us. The remaining pairs show negative values from −1.3 mG to −6.1 mG, corresponding to vectors of the magnetic field directed towards us. Five Zeeman pairs have spots polarized linearly with degrees from 8% to 48%.

2.2. *G48.990−0.299*

This source shows simple methanol maser emission consisting of two spots at velocity 71.5 km s^{-1}and 71.6 km s^{-1}and a brightness of 2.8 Jy beam^{-1}. The ex-OH emission is extended over the area 290×135 mas (1580×735 au) and appears in the velocity range from 66.7 km s^{-1}to 69.6 km s^{-1}. The maximum brightness is 2.6 Jy beam^{-1}. We do not notice any coincidence between the transitions in either velocity or position.

We identify four Zeeman pairs of ex-OH masers. Two eastern, blue-shifted groups have positive values of the magnetic field +2.3 mG and +2.7 mG and the vectors are directed away from us. Two western, red-shifted groups have negative values of the magnetic field −0.7 mG and −4.8 mG, and the vectors are directed towards us. The two brightest pairs have spots with linear polarization with degrees from 14% to 31%.

3. Discussion and Summary

G43 lies southwest of the large star-formation region W49N (De Buizer *et al.* 2021). At the south of the 6.7 and 6.035 GHz emission there are peaks of 20 μm and 37 μm continuum emission (De Buizer *et al.* 2021) and a few peaks of 3.6 cm radio-continuum emission (De Pree *et al.* 1997). Closer to the maser is a region of 226 GHz (1.3 mm) continuum emission (Miyawaki *et al.* 2022). This peak lies at a distance of ∼80 mas (∼876 au) towards the north from the brightest methanol maser spot. Close to the source an H$_{\rm II}$ region is also observed. The peak is ∼195 mas (∼2140 au) towards the west from the brightest methanol maser spot (Hu *et al.* 2016).

https://doi.org/10.1017/S1743921323002296 Published online by Cambridge University Press

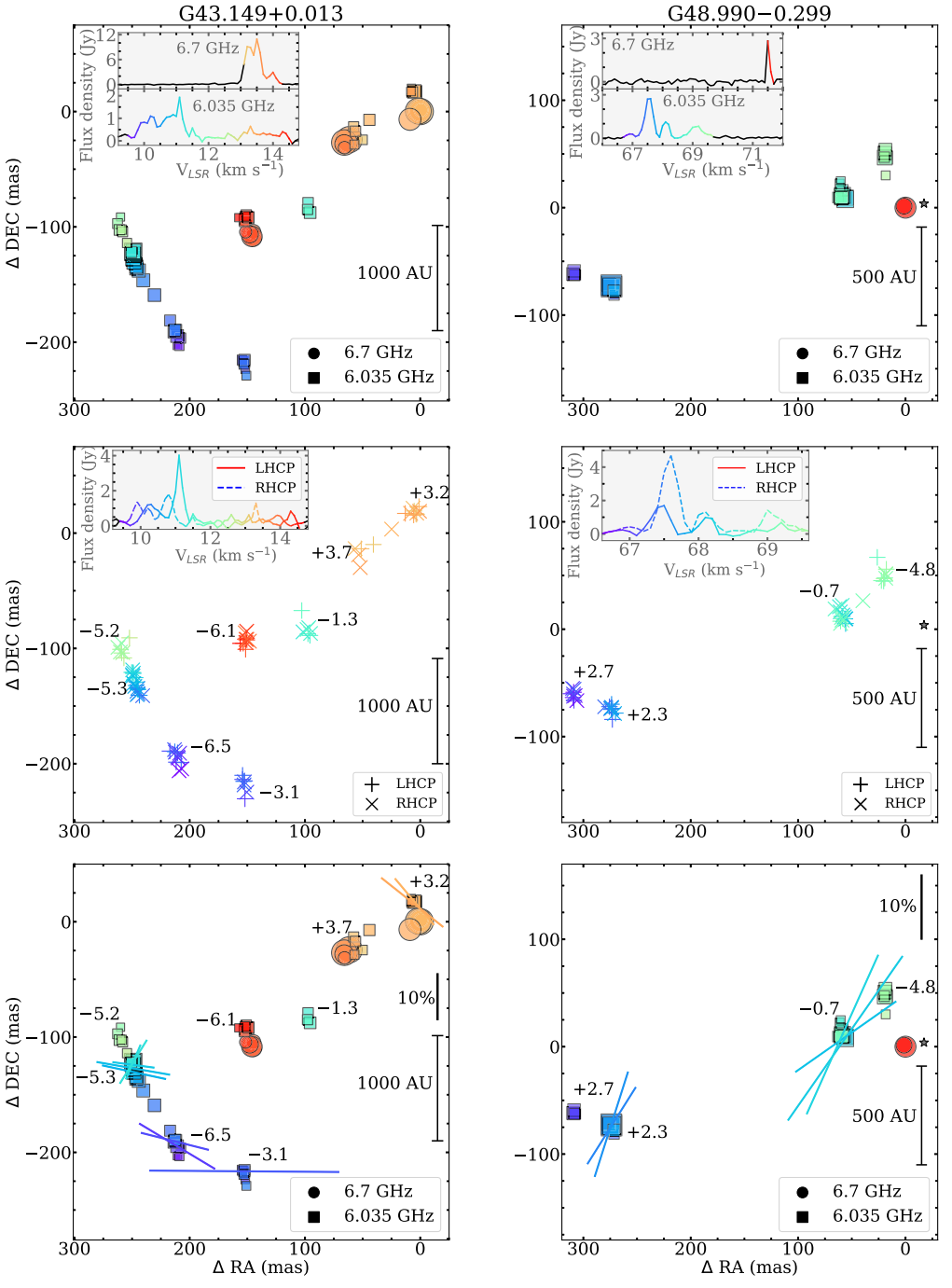

Figure 1. The 6.7 GHz methanol and 6.035 GHz ex-OH masers in G43.149+0.013 (left) and G48.990−0.299 (right). The size of the marks indicates the square root of the intensity, and the color indicates the V_{LSR} shown at the spectra. The grey star indicates the peak of H_{II} emission (Cooper *et al.* 2013). The (0,0) point corresponds to the brightest methanol maser spot. **Top:** Spectra and distributions of methanol (circle) and ex-OH (squares) maser spots. **Middle:** Spectra and distribution of left- and right-handed circular polarization (LHCP, RHCP). The numbers list the magnetic field strength in mG estimated based on the Zeemann splittings. **Bottom:** Distribution of maser spots with the values of magnetic field and percentage of linear polarization marked by colorful lines.

https://doi.org/10.1017/S1743921323002296 Published online by Cambridge University Press

The distributions of two kinds of masers suggest that the whole masing region has T_K below 70 K. Regions with only 6.035 GHz emission can come from higher gas density or lower dust temperatures. Considering that: 1) the ex-OH red-shifted masers indicate a stronger magnetic field (−6.1 mG), 2) B∼$n^{0.4}$, 3) ex-OH and methanol masers coincide, we can assume that the T_D is lower than T_K and it is the reason that the blue-shifted ex-OH masers avoid methanol masers. Furthermore, that indicates the red-shifted masers lie closer to the expected protostar traced by the 3.6 cm radio-continuum emission, and T_D exceed 100 K. In the region with blue-shifted masers, the dust temperature declined faster than the kinetic temperature with the distance from the protostar and declined below the kinetic temperature.

G48 is associated with the star-forming region W51 with H_{II} emission, with a peak lying close (∼17 mas corresponding to ∼94 au) to the brightest methanol maser spot (see Figure 1) (Cooper *et al.* 2013). Like in the previous source, H_{II} emission occurs close to the methanol maser emission but for that source without ex-OH counterparts which indicates the kinetic temperature above 70 K and dust temperature above 100 K in the red-shifted part of the source. The 6.035 GHz emission lay father from H_{II} emission so, as in the case of G43, we assume that the temperatures decrease (T_K and T_D) to the values that stop the occurrence of methanol masers.

Acknowledgements

e-MERLIN is a National Facility operated by the University of Manchester at Jodrell Bank Observatory on behalf of STFC, part of UK Research and Innovation. We acknowledge support from the National Science Centre, Poland through grant 2021/43/B/ST9/02008.

References

Baudry, A., Desmurs, J.F., Wilson, T.L., Cohen, R.J., 1997, *A&A*, 325, 255
Bartkiewicz A., Szymczak M., Cohen R.J., Richards A.M.S., 2005, *MNRAS*, 361, 623–632
Bartkiewicz A., Szymczak M., van Langevelde H.J., Richards A.M.S., Pihlström Y.M., 2009, *A&A*, 502, 155
Cooper, H.D.B., Lumsden, S.L., Oudmaijer, R.D., Hoare, M.G., Clarke, A.J., Urquhart, J.S., Mottram, J.C., Moore, T.J.T., Davies, B., 2013, *MNRAS*, 430, 1125–1157
Cragg, D.M., Sobolev, A.M., Godfrey, P.D. 2002, *MNRAS*, 331, 521–536
De Buizer, J.M., Lim, W., Liu, M., Karnath, N., Radomski, J.T., 2021, *ApJ*, 923, 198
De Pree, C.G., Mehringer, D.M., Goss, W.M., 1997, *ApJ*, 482, 307
Garay, G., Ramirez, S., Rodriguez, L.F., Curiel, S., Torrelles, J.M., 1996, *ApJ*, 459, 193
Green, J.A., Richards, A.M.S., Vlemmings, W.H.T., Diamond, P., Cohen, R.J., 2007, *MNRAS*, 382, 770–778
Kobak, A., Bartkiewicz, A., Szymczak, M., Olech, M., Durjasz, M., Wolak, P., Chibueze, J.O., Hirota, T., Eislöffel, J., Stecklum, B., Sobolev, A., Bayandina, O., Orosz, G., Burns, R.A., Kim, K.T. and van den Heever, S.P, 2023, *A&A*, 671, A135
Krumholz, M.R., Federrath, C., 2019, *Frontiers in Astronomy and Space Sciences*, 6, 7
Reid, M., Menten, K.M., Brunthaler, A., 2019, *ApJ*, 885, 131
Miyawaki, R., Hayashi, M., Hasegawa, T., 2022, *PASJ*, 74, 705–737
Szymczak, M., Kus, A.J., Hrynek, G., Kepa, A., Pazderski, E., 2002, *A&A*, 392, 277–286
Szymczak, M., Olech, M., Sarniak, R., Wolak, P., Bartkiewicz, A., 2018, *MNRAS*, 474, 219–253
Hu, B., Menten, K.M., Wu, Y., Bartkiewicz, A., Rygl, K., Reid, M.J., Urquhart, J.S., Zheng, X., 2016, *ApJ*, 833, 18
Yang, K., Chen, X., Shen, Z.Q., Li, X.Q., Wang, J.Z., Jiang, D.R., Li, J., Dong, J., Wu, Y.J., Qiao, H.H., 2019, *ApJS*, 241, 39